Food Hydrocolloids 100 (2020) 105357

Contents lists available at ScienceDirect

Food Hydrocolloids

journal homepage: www.elsevier.com/locate/foodhyd

Design of β-lactoglobulin micro- and nanostructures by controlling gelation through physical variables

Lívia S. Simões[a], João F. Araújo[a], António A. Vicente[a], Oscar L. Ramos[b,*]

[a] CEB, Center of Biological Engineering, University of Minho, Campus de Gualtar, 5710-057, Braga, Portugal
[b] CBQF, Centro de Biotecnologia e Química Fina, Escola Superior de Biotecnologia, Universidade Católica Portuguesa/Porto, Porto, 4202-401, Portugal

ARTICLE INFO

Keywords:
Purification
Bio-based structures
Globular proteins
Whey proteins
Protein interaction
Aggregation

ABSTRACT

β-lactoglobulin (β-Lg) is the major protein fraction of bovine whey serum and its principal gelling agent. Its gelation capacity enables conformational changes associated with protein-protein interactions that allow the design of structures with different properties and morphologies. Thus, the aim of this work was to successfully use β-Lg, purified from a commercial whey protein isolate, to develop food-grade micro- (with diameters between 200 and 300 nm) and nano- (with diameters ≤ 100 nm) structures. For this purpose, the phenomena involved in β-Lg gelation were studied under combined effects of concentrations (from 5 to 15 mg mL^{-1}), heating temperature (from 60 to 80 °C) and heating time (from 5 to 25 min) for pH values of 3, 4, 6 and 7. The effects of such conditions on β-Lg structures were evaluated and the protein was fully characterized in terms of size, polydispersity index (PDI) and surface charge (by dynamic light scattering – DLS), morphology (by transmission electron microscopy - TEM) and conformational structure (circular dichroism, intrinsic and extrinsic fluorescence). Results have shown that β-Lg nanostructures were formed at pH 3 (with diameters between 12.1 and 22.3 nm) and at 7 (with diameters between 8.9 and 35.3 nm). At pH 4 structures were obtained at macroscale (i.e., ≥ 6 μm) for all β-Lg concentrations when heated at 70 and 80 °C, independent of the time of heating. For pH 6, it was possible to obtain β-Lg structures either at micro- (245.0 – 266.4 nm) or nanoscale (≤ 100 nm) with the lowest polydispersity (PDI) values (≤ 0.25), in accordance with TEM analyses, for heating at 80 °C for 15 min. Intrinsic and extrinsic fluorescence data and far-UV circular dichroism spectra measurements revealed conformational changes on β-Lg structure that support these evidences. A strict control of the physical and environmental conditions is crucial for developing β-Lg structures with the desired characteristics, thus calling for the understanding of the mechanisms of protein aggregation and intermolecular interaction when designing β-Lg structures with novel functionalities.

1. Introduction

Bovine β-lactoglobulin (β-Lg) is a globular protein obtained from milk and the main fraction of whey proteins (ca. 50 % of its protein content), widely used as functional and nutritional ingredient in food, cosmetic and pharmaceutical industry (Pereira et al., 2015; Rodrigues et al., 2015). Whey proteins are obtained from whey, which is a by-product of cheese production, relatively inexpensive and classified as a GRAS (generally regarded as safe) material (Madalena et al., 2016).

The interest in β-Lg from both the scientific community and food and pharmaceutical industries is essentially due to its high nutritional value as a consequence of the rich level of amino acids, resistance to proteolytic degradation in the stomach, biological (e.g., digestibility, sensory characteristics and high biological value) properties, and gelation capacity, which is particularly important since it allows the formation of structures with different properties and morphologies (Ramos et al., 2012).

Thermally induced gelation usually consists in the unfolding of polypeptide chains of protein in native state with concomitant exposure of initially buried hydrophobic amino acid residues, and subsequent self-aggregation of protein molecules through physical (electrostatic and hydrophobic) and chemical (disulphide) interactions (Delahaije, Wierenga, Giuseppin, & Gruppen, 2015; Teng, Xu, & Wang, 2015). The extent and behavior of protein aggregation depends on several physical conditions such as heating temperature, time of heating, pH, protein concentration and ionic strength (Ramos et al., 2015), and can result in different structures with various sizes, shapes, morphologies and charges.

* Corresponding author. CBQF, Centro de Biotecnologia e Química Fina, Escola Superior de Biotecnologia, Universidade Católica Portuguesa/Porto, Porto, 4202-401, Portugal.
E-mail address: os.silva.ramos@gmail.com (O.L. Ramos).

https://doi.org/10.1016/j.foodhyd.2019.105357
Received 26 February 2019; Received in revised form 26 July 2019; Accepted 2 September 2019
Available online 04 September 2019
0268-005X/

Recent publications have been focused on understanding the structural gelation and aggregation of β-Lg, but only under limited physical and environmental conditions. For instance, Dombrowski, Gschwendtner, and Kulozik (2017) evaluated the specific role of pH (from 3 to 11) at fixed β-Lg concentration (1.0 %), temperature (80 °C), and time of heating (90 min) on surface charge and structural properties (i.e., particle size and surface hydrophobicity) of heat-induced β-Lg aggregates. Dombrowski, Johler, Warncke, & Kulozik (2016) assessed the specific effects of salt type and concentration (NaCl and $CaCl_2$, 0 – 300 mmol L^{-1}) on the interaction behaviour of β-Lg molecules at fixed protein concentration (0.1 %) and pH (pH = 6.8) conditions in view of their surface and foaming properties using a multiscale approach. Fan et al. (2019) studied the influences of mannosylerythritol lipid-A at concentration ranging from 0 to 5.0 mg mL^{-1} on the structure formation and functional properties β-Lg aggregates at fixed β-Lg concentration (2.0 %), temperature (85 °C), and pH (5.8) conditions. Delahaije et al. (2015) investigated the kinetics of heat-induced aggregation and the size/density of β-Lg under various pH (5, 6 and 7), ionic strengths (10, 40 and 90 mmol L^{-1} of NaCl) and protein concentrations (1, 2, 5 and 10 g L^{-1}); these conditions were, however, tested isolated. Perez, Andermatten, Rubiolo, and Santiago (2014) studied the impact of a narrow pH range (6.5, 7.0 and 7.5) and temperature of heating (15, 30, 45 and 60 min) on the development of β-Lg aggregates as carriers systems, at fixed protein concentration (1.0 %) and heating temperature (85 °C) conditions. Despite all these studies on β-Lg structures formation and discussions about the structural modifications over distinct conditions, there is limited (or even inexistent data) about how all these conditions applied in a combined way affect the denaturation and aggregation of β-Lg, and thus the size, morphology, shape, and stability of developed structures. Evidences exist showing that the combination of some physical conditions impact differently (when compared with those effects separately) the extent of aggregation, and thus the final properties and functionalities of resulting structures (Ramos et al., 2017; Ramos et al., 2014). Therefore, the full understanding of the mechanisms behind the protein gelation that lead to structural conformational changes and thus to the formation of different structures is crucial. However, β-Lg at high purity levels is commercially available only at high cost, thus obtaining it from cheaper commercial protein powders may represent a more suitable and feasible solution. In this context, a pure β-Lg fraction was obtained, during this study, from a commercial whey protein isolate based on an established procedure. This step allowed us to obtain the quantity of β-Lg needed to perform all the experiments at low cost by using an inexpensive source, while promoting the valorization of a whey protein product with relatively low commercial value. Then, the main physicochemical properties of purified β-Lg was compared to a commercial β-Lg to assess their similarity. Thus, purified β-Lg was extensively characterized through a complementary set of techniques and the protein structural (conformational) changes were assessed upon thermal gelation, under combined physical and environmental conditions (various β-Lg concentrations, heating temperatures and times) at distinct pH values (3 – 7), to design food-grade micro- (200 – 300 nm) and nanostructures (≤ 100 nm). The small size of micro- and nanostructures can impart significant changes to physicochemical properties, among them a high surface/volume ratio, smaller pore size and increase in the solubility when compared with macroscale structures formed from the same proteins (Aklakur, Rather, & Kumar, 2016; Monteiro et al., 2016). In this regard, the effect of aforementioned physical conditions on β-Lg structures were evaluated in order to provide detailed information about the specific conditions that lead to the formation of β-Lg structures at micro- and nanoscale, which hold potential to be used as delivery systems for bioactive compounds.

2. Material and methods

2.1. Feedstocks and chemicals

Whey Protein Isolate (WPI) powder (Lacprodan DI-9212), kindly supplied by Arla Foods Ingredients (Viby, Denmark), has in a total protein content of 91 % (in dry weight), moisture content of ca. 6 % and vestiges of lactose (max. 0.5 %) and fat (max. 0.2 %). The amount of proteins considered to be in their "native" state was 85 % of the total protein content. β-Lg was obtained as a commercial lyophilized powder from bovine milk (Sigma L0130), containing variants A and B (Molecular weight (Mw) = 36.0 kDa) with a purity of 90 % (L0130). Tris(hydroxymethyl)aminomethane, ammonium persulfate (APS), Coomassie Brilliant Blue (R-250), bromophenol blue and tetramethylethylenediamine were purchased from Sigma Aldrich (St. Louis MO, USA). Sodium hydroxide, phosphoric and acetic acids were obtained from Merck (Merck KGaA, Darmstadt, Germany). Hydrochloric acid, glycine and monosodium phosphate were purchased from Panreac (Barcelona, Spain), whereas sodium phosphate dibasic and methanol were obtained from Chem-Lab (Zedelgem, Belgium). Acrylamide was purchased from Bio-Rad (California, USA) and glycerol was obtained from Himedia (Mumbai, India). All other chemicals used in this study were reagent-grade or higher, and were used without further purification.

2.2. β-Lg purification method

Purified β-Lg was obtained from WPI by using the salting out method as described by Maté and Krochta (1994) with modifications according with Konrad, Lieske, and Faber (2000). WPI powder (15 % w/w) was dispersed in distilled water and the pH of the solution was adjusted to 2.0 by addition of 2 mol L^{-1} with HCl. Subsequently, 7 % (w/w) of NaCl was added to promote the separation of β-Lg from other proteins in the precipitate. The precipitation process was held for 20 min at room temperature (i.e., 25 °C). The solution was centrifugated (Sigma 4K15, Germany) at 13 000 × *g*, at 4 °C for 15 min. After separating phases, the sediment was discarded. The ultrafiltration with diafiltration of supernatant was performed to separate the β-Lg from salt. The process was carried out using Pelicon® ultrafiltration cassettes with membrane cut-off Mw = 10 kDa, which the retentate (β-Lg, salt and water) was recycled to the feed tank and make-up water was added; the permeate (salt and water) was eliminated. The ultrafiltration process was repeated until the feed tank electrical conductivity reaches 0.9 mS cm^{-1}. This value ensures the lower amount of salt in the resulting solution. β-Lg was freeze dried to obtain a lyophilized powder. The purity and conformational properties of purified β-Lg were compared with commercial β-Lg lyophilized powder from Sigma. For this purpose, both protein solutions were prepared by dispersing 10 mg mL^{-1} of β-Lg powder (Dombrowski et al., 2016; Donato, Schmitt, Bovetto, & Rouvet, 2009; Kosters, Wierenga, De Vries, & Gruppen, 2011; Schmitt et al., 2009) in 25 mmol L^{-1} sodium phosphate buffer at pH 6. The pH of solutions was adjusted with 0.5 mol L^{-1} of H_3PO_4 or 1 mol L^{-1} of NaOH, as necessary. The solutions were then stirred continuously with a rotation speed of 400 rpm, for 2 h at room temperature (ca. 25 °C). Afterward, β-Lg solutions were stored at refrigeration temperature (5 °C) overnight to ensure the full rehydration of protein. The β-Lg solutions were then filtered through a 0.2 μm membrane filter (VWR International, USA) to remove any protein aggregates or impurities. Subsequently, β-Lg morphology, purity, secondary structure and conformational state properties were evaluated for both commercial and purified β-Lg, through dynamic light scattering, SDS-PAGE, turbidity, circular dichroism, intrinsic and extrinsic fluorescence analyses and then comparisons were drawn.

2.3. Measurements

2.3.1. Particle size, polydispersity index, and ζ-potential

Samples of β-Lg were characterized in terms of particle size, polydispersity index (PDI) and ζ-potential by Dynamic Light Scattering (DLS) apparatus (Zetasizer Nano ZS, Malvern Instruments, UK) equipped with He–Ne laser at a wavelength of 633 nm, at 25 °C (Bourbon, Pinheiro, Cerqueira, & Vicente, 2016). Particle size was determined by the method of cumulants fit and was translated into average particle diameters (Z-value) using the Stokes-Einstein relationship (Rodrigues et al., 2015). PDI emerged from cumulants analysis of the measurements and describes the width or the relative variance of the particle diameter distribution. The ζ-potential determines the charge at the surface of the structure and was performed with an angle of 17° (Madalena et al., 2016). Samples (1.5 mL) were poured into disposable sizing cuvettes with a path length of 10 mm for particle size and PDI analyses, and into a folded capillary cell for ζ-potential measurements. All measurements were carried out at 25 °C and the results reported as the average ± standard deviation of at least three replicates.

2.3.2. Turbidity

The turbidity of β-Lg solutions (4 mL) prepared at 10 mg mL^{-1} was evaluated using a double-beam UV/visible spectrophotometer at 500 nm (V-560, Jasco Inc., Tokyo, Japan). The measurements were made at room temperature (ca. 25 °C) according with the procedure reported by Pereira et al. (2015) resorting to a 10 mm path length cuvette, and with 25 mmol L^{-1} sodium phosphate sodium buffer as blank. The measurements were performed in triplicate and experimental values are presented as the average ± standard deviation.

2.3.3. Intrinsic fluorescence

Intrinsic fluorescence measurements of β-Lg dispersions from 5 to 15 mg mL^{-1} were obtained at ambient temperature (ca. 25 °C) resorting to a spectrofluorimeter (Jasco FP6200, Tokyo, Japan) equipped with a standard thermostated cell holder and a 10 mm path length quartz cuvette (Hellma Analytics, Germany). The excitation wavelength was set at 295 nm to quenching tryptophan (Trp) fluorescence (Madadlou, Floury, Pezennec, & Dupont, 2018) and the emission spectra were recorded between 300 and 405 nm, and fluorescence intensities were recorded every 2.25 nm. Spectra were baseline-corrected by subtracting blank spectra (i.e. 25 mmol L^{-1} sodium phosphate buffer) according the procedure adopted by Monteiro et al. (2016) and normalized with unheated β-Lg. The maximum intrinsic fluorescence intensity was given as the average of nine successive measurements.

2.3.4. Extrinsic fluorescence

The extrinsic fluorescence of β-Lg dispersions from 5 to 15 mg mL^{-1} was determined by fluorescence spectroscopy (Jasco FP6200, Tokyo, Japan) using 8-anilinonaphtalene-1-sulfonic acid ammonium salt (ANS) (Sigma-Aldrich, St. Louis, EUA) as the hydrophobic probe, according to the methodology adopted by Wang, Zhong, and Hu (2013) with a few modifications. The β-Lg solutions were incubated at 25 °C prepared ANS solution (at 1.36 mmol L^{-1} in methanol) for 10 min in the dark before the analysis. The resulting solution was excited at 370 nm and emission was collected between 400 and 600 nm at ambient temperature (ca. 25 °C), using a 10 mm path length quartz cuvette. Spectra were baseline-corrected by subtracting blank spectra (i.e., 25 mmol L^{-1} sodium phosphate buffer and ANS solution). Micro- and nanostructures maximum fluorescence intensity values were normalized by the lowest value corresponding to the unheated β-Lg. The maximum ANS binding fluorescence intensity was given as the average of nine successive measurements.

2.3.5. Circular dichroism

The secondary structure content of β-Lg and the effect of heat treatment were evaluated by circular dichroism (CD). CD spectra were obtained resorting to a Jasco J-1500 spectropolarimeter (Jasco International Co, Japan). For far-UV experiments, samples in appropriate dilution and spectra were recorded at 25 °C, under constant nitrogen flush, using a quartz cuvette with an optical path length of 1.0 mm (Hellma Analytics, Germany), from 190 nm to 260 nm wavelength range with data pitch of 1.0 nm and accumulation of 3 scan, following the procedure used by Bourbon et al. (2016). The CD baseline scan was recorded using a standard solution of 25 mmol L^{-1} sodium phosphate buffer and then subtracted to scans from β-Lg solutions.

2.3.6. Native polyacrylamide gel electrophoresis (Native–PAGE)

In order to compare the integrated intensities of β-Lg bands, samples were analyzed using Native-PAGE or "nondenaturing" gel electrophoresis. Native-PAGE analyses were carried out using the Mini-Protean II dual slab cell system equipped with a PAC 300 power supply (Bio-Rad Laboratories, Hercules, CA, USA) (Bourbon et al., 2016). The resolving and stacking gel contained 12.5 and 3.5 % of polyacrylamide, respectively. Non-reducing loading buffer of tris(hydroxymethyl)aminomethane, 0.5 mol L^{-1} at pH 6.8, 50 % of glycerol and 0.02 % of bromophenol blue was mixed with β-Lg samples. The gels were stained with Coomassie Brilliant Blue (R-250) solution, maintained overnight in 50 % and 10 % of methanol and acetic acid solutions, respectively. Then, gels were destained with 30 % and 7 % of methanol and acetic acid solutions, respectively (Rodrigues et al., 2015). Standard marker protein PageRuler Unstained Broad Range Protein Ladder (Thermo Scientific) was employed to identify samples by their molecular weight.

2.3.7. Fast protein liquid chromatography

β-Lg protein solutions were resolved and quantified by gel filtration chromatography using a Superdex™ 200 10/300 GL column, connected to a fast protein liquid chromatography (FPLC) AKTA-purifier system (GE). β-Lg lyophilized solutions (from Sigma) with concentrations ranging from 5 to 15 mg mL^{-1} were used to prepare a calibration curve, then 10 mg mL^{-1} of β-Lg purified samples were analyzed.

The protein samples were then centrifuged at 20 000 × *g* for 1 h at 25 °C, using a Sorvall centrifuge, and 5 mL of the clarified liquid was carefully collected and filtered through 0.22 μm filters prior to separation. The eluent was also filtered (0.22 μm) and degassed under vacuum for 1 h before testing. Samples (100 μL) were injected into the column and eluted using 0.05 mol L^{-1} of sodium phosphate buffer (pH 7) containing 0.2 g L^{-1} of sodium azide, as preservative, at a flow rate of 0.5 ml ml^{-1} under a pressure of 1.5 – 2.0 MPa. Identification (through similarity of retention times – RT) and quantification (by integration of peak area of chromatograms) of the β-Lg present in the eluate was monitored at 280 nm following the procedure previously described by Ramos et al. (2012). All measurements were performed at least in duplicate.

2.3.8. Transmission electron microscopy

Transmission electron microscopy (TEM) imaging of β-Lg micro- and nanostructures was conducted on a Zeiss EM 902A (Thornwood, N.Y., USA) microscope at accelerating voltages of 50 and 80 kV. A drop of sample dispersion was deposited onto a carbon support film mounted on a TEM copper grid (Quantifoil, Germany).

The excess of solution was removed after 2 min using a filter paper and the grid let for air-drying. The samples were then negatively stained with uranyl acetate (2% w/w) (Merck, Germany) for 15 s. The grid was finally air dried at room temperature before introducing it in the electron microscope. These conditions were used based in procedures usually adopted by our research group (Monteiro et al., 2016; Bourbon et al., 2015; Pinheiro et al., 2015).

2.4. Experimental design

Box-Behnken statistical experimental design was used to evaluate

Table 1
Independent variables and their levels in Box-Behnken experimental design for pH values 3, 4, 6 and 7.

Independent variables	Levels		
	Low	Medium	High
X_1 (Heating temperature, °C)	−1 (60)	0 (70)	+1 (80)
X_2 (β-Lg concentration, mg mL^{-1})	−1 (5)	0 (10)	+1 (15)
X_3 (Holding time, min)	−1 (5)	0 (15)	+1 (25)

the effect of heating temperature (X_1), β-Lg concentration (X_2) and holding time (X_3) (independent variables), upon particle size (Y_1), polydispersity index (Y_2), intrinsic fluorescence (Y_3) and extrinsic fluorescence (Y_4) intensities (dependent variables), on the development of optimized β-Lg micro- and nanostructures at pH 3, 4, 6 and 7. A 3-factor, 3-level design was used because it was the most appropriated for exploring quadratic response surfaces and constructing second order polynomial models for optimization, thus allowing the use of less experiments. The experimental design encompasses the repetition of center points and the set of points lying at the midpoints of each edge of the multidimensional cube that defines the region of interest. The pH values were selected based on the isoelectric point (pI) of β-Lg (Teng et al., 2015). As shown in Table 1, the independent variables and levels (i.e., low, medium and high) were selected based in previous results from screening experiments. The relatively narrow range of protein concentrations evaluated was based on preliminary results (data not shown) obtained for 0.5, 1, 5, 10, 20, 40 and 60 mg mL^{-1} of β-Lg. The design matrix was performed in 15 trials flowing the procedure adopted by Monteiro et al. (2016).

2.5. Development of β-Lg micro- and nanostructures

To study the effects of β-Lg concentration, temperature and time of heating upon the formation of protein micro- and nanostructures at different pH values, the solution pH was adjusted to 3, 4, 6 and 7 with 0.5 mol L^{-1} of H_3PO_4 or 1 mol L^{-1} of NaOH, as appropriate. Micro- and nanostructures were formed by dispersing 5, 10 and 15 mg mL^{-1} of β-Lg purified powder in 25 mmol L^{-1} sodium phosphate buffer at pH 3, 4, 6 and 7. The solutions were then stirred continuously with a rotation speed of 400 rpm, for 2 h at room temperature (ca. 25 °C). Afterward, β-Lg solutions were stored at refrigeration temperature (5 °C) overnight to ensure the full rehydration of protein. The β-Lg solutions (5 mL) were then filtered through a 0.2 μm membrane filter to remove any protein aggregates or impurities and were placed into cylindrical screw-capped glass tubes (100 mm total length and diameter of 20 mm). Heat treatments at different temperatures (i.e., 60 – 80 °C) and times (i.e., 5 – 25 min) were applied through a temperature controlled water bath (MR Hei-Tec + Pt 1000, Heidolph) with samples continuously stirred with magnetic agitation at a rotation speed of 400 rpm. After the heat treatment, the resulting solutions were cooled in ice for 10 min. β-Lg structures were characterized using the techniques described before. Unheated and native β-Lg suspensions were used as control samples.

2.6. Statistical analyses

All statistical analyses involving experimental data were performed using Statistica package software version 10.0.228.8 (StatSoft Inc., Tulsa, OK, USA). Statistical significance (at $p \leq 0.05$) was determined using ANOVA one-way, followed by Tukey's tests. Unless otherwise stated, all experiments were run at least in triplicate.

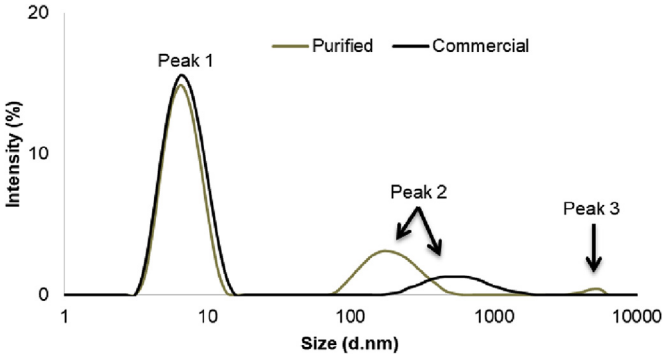

Fig. 1. Typical particle size distribution curve (by intensity) obtained for purified and commercial unheated β-Lg, prepared at 10 mg mL^{-1} and pH 6.

3. Results and discussion

3.1. β-Lg purification

In order to evaluate the purification process efficacy using an established method, purified β-Lg was extensively characterized in terms of physicochemical properties and the results obtained were compared with the commercial β-Lg at the same conditions. Particle size distribution results of both β-Lg (purified and commercial) are presented in Fig. 1, showing a polymodal distribution of unheated β-Lg for both purified and commercial protein with two predominant peaks: peak 1 with maximum between 2 and 10 nm, which is attributed to non-aggregated proteins, and peak 2 associated to native β-Lg aggregates. It is also possible to observe a third peak, but only for purified β-Lg, which can be attributed to strands and clumps of small globular aggregates as result of the purification process. This behavior was somehow expected and has been previously reported elsewhere (Rodrigues et al., 2015).

In particular for peak 1, measurements revealed a particle size and PDI values of 8.89 ± 0.06 nm and of 0.363 ± 0.004, respectively, for purified β-Lg, and of 6.83 ± 0.16 nm and 0.169 ± 0.031, respectively, for commercial β-Lg. Statistically significant differences ($p \leq 0.05$) were obtained between purified and commercial β-Lg for both parameters. These differences may be due to distinct intensities of intrinsic forces (i.e., electrostatic interactions, hydrogen and disulphide bonds, hydration and hydrophobic effects) involved on the stability of the tertiary folds (Ramos et al., 2014). On the other hand, regarding protein turbidity, purified and commercial β-Lg displayed statistically similar values ($p > 0.05$) – 0.0023 ± 0.0003 and 0.0028 ± 0.0002, respectively – suggesting that both proteins are in identical "native" state, i.e., the content of aggregated proteins is very small.

In order to evaluate the protein stability promoted by electrostatic interactions, ζ-potential values were determined. Purified and commercial β-Lg solutions showed a statistically similar ($p > 0.05$) ζ-potential of −9.34 ± 0.71 mV and −7.93 ± 0.99 mV, respectively. These values suggest that β-Lg, in its native state, is a relatively unstable system under the measured conditions. According to Ghalandari, Divsalar, Saboury, and Parivar (2015) and von Staszewski et al. (2012), a colloidal system is considered stable when displaying ζ-potential values above +30 mV or below −30 mV, thus meaning that the charge between particles (i.e., repulsion) is enough to prevent aggregation. The protein conformational changes are widely accessed through intrinsic tryptophan fluorescence measurements (Stănciuc, Aprodu, Râpeanu, & Bahrim, 2012; Vivian & Callis, 2001). This analysis was performed in order to investigate if there is any change in protein structure and dynamics between both β-Lg proteins. The main responsible for β-Lg fluorescence are two tryptophan (Trp) residues (i.e., Trp-19 and Trp-61), being the intrinsic fluorescence of the protein mostly attributed to Trp-19, since it is found in the hydrophobic calyx of β-Lg, while Trp-61 is located in an external loop, close to protein surface (Simion et al.,

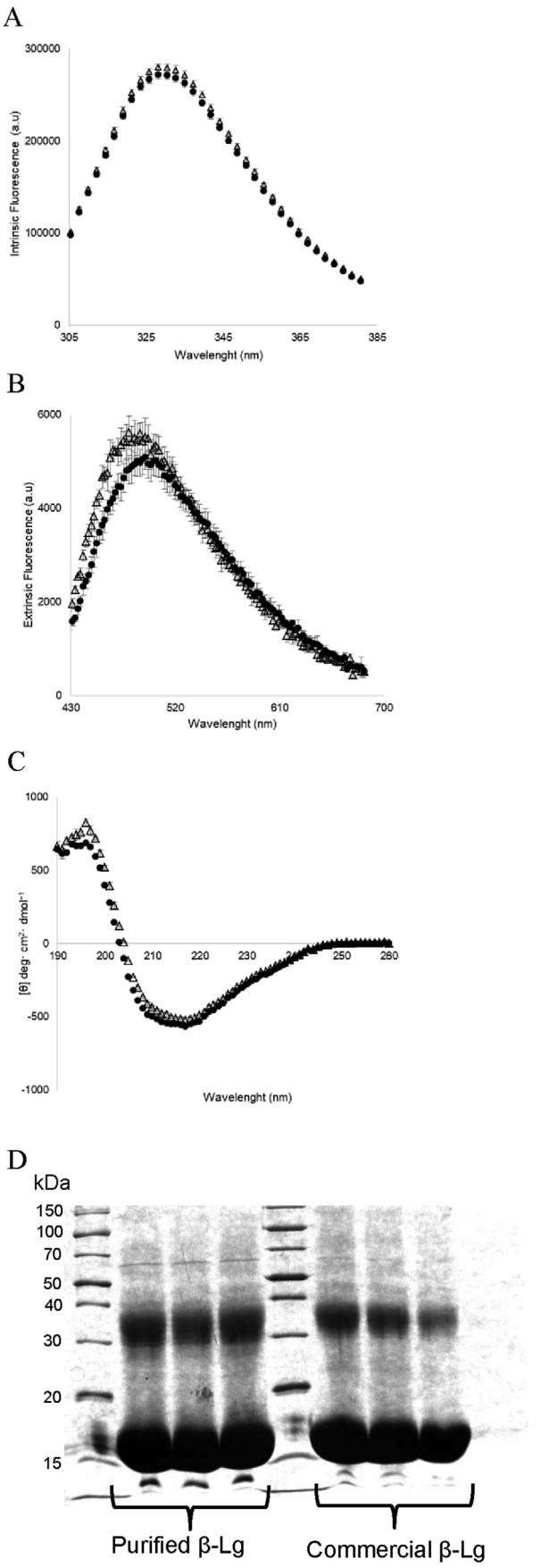

Fig. 2. Comparison between (•) purified β-Lg and (Δ) commercial β-Lg solutions. (A) Intrinsic fluorescence emission spectra at 295 nm; (B) extrinsic fluorescence emission spectra at 370 nm; (C) Far-UV CD spectra; (D) Native-PAGE. Standard deviation is represented by error bars.

2015). Fig. 2A presents the intrinsic fluorescence intensity results of purified and commercial β-Lg solutions exhibiting both a maximum intensity peak at 333 nm. Typically, β-Lg has a maximum intrinsic fluorescence emission around 335 nm (Diarrassouba, Liang, Remondetto, & Subirade, 2013), so this result corresponds to a blue shift behavior, thus suggesting that chromophoric groups of both samples are more buried in the interior of protein, i.e., hydrophobic groups were protected from the aqueous environment (Perez et al., 2014).

The extrinsic fluorescence, by means of the ANS fluorescent probe that binds to hydrophobic sites of proteins, provide information about changes of protein-probe interactions and on variation of the accessible hydrophobic areas (Stănciuc et al., 2012). Fig. 2B shows a higher intensity ($p \leq 0.05$) in the peak emission of commercial β-Lg than that of purified β-Lg, thus suggesting that the latter β-Lg was less prone to bind to ANS than commercial ones. Probably, the purification process, which has resulted in a significant higher particle size of β-Lg as mentioned before, led for one hand, to a lower surface-area-to-volume ratio to react with ANS, and for other hand to less change at the conformational level, thus making these hydrophobic groups less exposed to ANS (Perez et al., 2014; Simion et al., 2015). Circular dichroism (CD) spectroscopy provides information and consequently less accessible on the main secondary structural elements (i.e., α-helix, β-sheet and coil) of proteins, through measurement of polarized light absorbed by peptide bonds (Monteiro et al., 2016). The α-helix structure is characterized by displaying an intense and positive band at 190 nm and negative peaks at 208 and 220 nm, the β-sheet structure typically presents a negative peak with a minimum in the 215 nm region, while random coil structures display a positive peak close to 215 nm and a negative one near to 200 nm (Furtado, Pereira, Vicente, & Cunha, 2018). The values recorded from 190 to 260 nm for purified and commercial β-Lg in native state is depicted in Fig. 2C, displaying similar spectra in terms of CD intensity and shape. Moreover, the scans exhibited a negative dichroic peak with a minimum at 217 nm (i.e., in the 215 nm region), indicating that the secondary structure of both purified and commercial β-Lg are rich in β-sheet (Estévez et al., 2017; Fan, Zhang, Yokoyama, & Yi, 2017; Yi, Lam, Yokoyama, Cheng, & Zhong, 2014).

Electrophoresis analysis from Fig. 2D shows two sets of results, composed by three lanes, where it is possible to observe an identical profile for purified and commercial β-Lg. Given that unbound dye is removed by long gel washing gel process, the amount of bound dye is proportional to the protein concentration in the sample (Rodrigues et al., 2015). Both purified and commercial β-Lg samples were characterized by the presence of two high molecular weight bands. The higher molecular weight band with molecular mass between 30 and 40 kDa indicates the presence of β-Lg in dimer form, whereas the lower molecular weight band with molecular mass between 15 and 20 kDa corresponds to β-Lg in monomer form, in agreement with previous research on β-Lg (Halder, Chakraborty, Das, & Bose, 2012; Madalena et al., 2016).

Fast Protein Liquid Chromatography (FPLC) is the preferential methodology employed for separation and quantification of proteins, essential due to the good resolution and low variability associated to this technique (Ramos et al., 2012). In this regard, FPLC was used to compare both purified and commercial β-Lg in terms of protein content. For this purpose, an appropriate calibration curve ($y = 120.1x + 2.8$) was obtained with $R^2 = 0.999$ using several concentrations of commercial β-Lg, where y is protein content and x is β-Lg concentration. Peak area integration showed statistically similar ($p > 0.05$) concentration values of 123.10 ± 1.90 and 120.70 ± 0.80 AU mL^{-1} for purified and commercial β-Lg samples, respectively, prepared at 10 mg mL^{-1}.

3.2. Development of micro- and nanostructures

In order to understand the influence of β-Lg concentration and

Table 2
Experimental responses of particle size distribution, polydispersity index (PDI), intrinsic fluorescence (IF) and extrinsic fluorescence (EF) intensities for the Box-Behnken design.

pH	X_1 (Heating temperature, °C)	X_2 (β-Lg concentration, mg mL^{-1})	X_3 (Holding time, min)	Particle size (d.nm)	PDI	Normalized IF (a.u)	Normalized EF (a.u)
3	60	10	5	12.1	0.55	1.04	1.15
		15	15	12.6	0.58	1.02	1.92
		5	15	12.3	0.55	0.93	0.80
		10	25	13.1	0.59	0.88	0.96
	70	5	5	15.2	0.68	0.82	1.25
		15	5	13.5	0.62	1.00	1.04
		10	15	12.7	0.58	0.98	1.05
		10	15	12.6	0.58	0.95	0.79
		10	15	13.5	0.62	0.97	1.08
		5	25	17.0	0.75	0.84	0.87
		15	25	13.7	0.63	0.99	0.89
	80	10	5	16.2	0.73	0.95	1.24
		15	15	17.0	0.76	0.97	1.47
		5	15	22.3	0.99	0.81	1.14
		10	25	21.3	0.92	0.94	1.99
4	60	10	5	40.7	0.76	1.05	0.96
		15	15	44.1	0.98	1.02	1.81
		5	15	48.4	0.85	1.02	0.68
		10	25	45.0	0.93	1.00	1.75
	70	5	5	1914.3	0.51	1.01	1.12
		15	5	379.1	0.66	0.98	3.91
		10	15	2444.5	0.40	1.04	3.18
		10	15	3158.5	0.98	1.04	2.79
		10	15	3622.5	0.76	1.00	2.67
		5	25	1426.0	0.53	0.98	2.09
		15	25	2031.6	0.43	1.05	4.41
	80	10	5	> 6000	1.00	1.91	8.32
		15	15	> 6000	1.00	2.80	15.00
		5	15	> 6000	1.00	2.39	5.64
		10	25	> 6000	1.00	0.79	9.49
6	60	10	5	8.6	0.36	1.07	0.89
		15	15	8.9	0.36	1.38	1.13
		5	15	9.8	0.43	1.05	0.67
		10	25	8.7	0.36	1.12	0.90
	70	5	5	10.1	0.44	0.97	0.56
		15	5	10.1	0.42	1.51	1.21
		10	15	11.3	0.48	1.06	1.32
		10	15	13.2	0.56	1.09	1.06
		10	15	12.9	0.55	1.07	1.07
		5	25	13.2	0.58	1.01	0.67
		15	25	14.6	0.57	1.53	1.38
	80	10	5	84.8	0.34	4.67	13.72
		15	15	131.5	0.20	6.73	16.91
		5	15	78.1	0.25	4.42	8.28
		10	25	126.9	0.18	4.90	13.74
7	60	10	5	8.9	0.39	1.05	0.83
		15	15	12.2	0.53	1.05	0.78
		5	15	10.1	0.46	1.04	0.93
		10	25	13.3	0.56	1.00	0.84
	70	5	5	10.6	0.48	1.96	0.94
		15	5	13.3	0.56	0.99	0.79
		10	15	16.0	0.58	1.12	1.04
		10	15	16.5	0.59	1.08	1.04
		10	15	14.9	0.55	1.13	1.14
		5	25	16.9	0.64	1.07	1.28
		15	25	26.5	0.27	1.19	2.22
	80	10	5	33.1	0.38	1.27	2.27
		15	15	34.5	0.16	3.66	9.35
		5	15	21.6	0.59	1.20	1.75
		10	25	35.3	0.14	3.91	10.95

thermal treatment on the formation of micro- and nanostructures, various combined effects (including different concentrations of β-Lg, heating temperatures and times) were carried out to induce protein aggregation. An experimental design, shown in Table 2, was used to evaluate the combined effect of three β-Lg concentrations (5, 10 and 15 mg mL^{-1}), three temperatures (60, 70 and 80 °C), and three holding times (5, 15 and 25 min) on the particle size distribution, polydispersity index, and intrinsic and extrinsic fluorescence intensity of β-Lg solutions prepared at four different pH values (3, 4, 6 and 7).

These results show that performing the β-Lg gelation process in different combinations of environmental conditions allows obtaining β-Lg structures at nanoscale (i.e., with particle sizes below 50 nm), by changing pH to 3 and 7, independently of the protein concentration (5 – 15 mg mL^{-1}), heating temperature (60 – 80 °C) and holding time (5 – 25 min) used. This could be related to the fact that bovine β-Lg at pH values $\leq$ 3 and $\geq$ 7 exists as a monomer due to the intermolecular electrostatic repulsions that govern protein interactions at those pH values, thus leading to the formation of low particle size structures under those conditions (Diarrassouba et al., 2013; Ramos et al., 2015). Based on this, we believe that β-Lg structures with small particle sizes

(i.e., ≤ 50 nm) can be obtained at pH values far from β-Lg's pI (i.e., 4.6) (Schmitt et al., 2009), since at these conditions the protein is governed by electrostatic repulsions that hamper the aggregation process (Dombrowski et al., 2017).

Regarding fluorescence intensity, at pH 3 for all tested conditions and at pH 7 for heating temperatures of 60 °C and 70 °C, β-Lg structures were characterized by relatively low intrinsic and extrinsic fluorescence intensities with maxima of 1.96 and 2.22 (Table 2), respectively. Concerning the structural conformation, the low intrinsic fluorescence intensity obtained suggests that either β-Lg was not completely unfold or the tryptophan residue was not sufficiently exposed, being buried within the native protein structure (Ramos et al., 2015). Regarding extrinsic fluorescence intensity, determined by means of ANS fluorescence probe, it was possible to verify a low accessibility of ANS to hydrophobic areas of β-Lg, translated by a low extrinsic fluorescence intensity emitted (Schmitt et al., 2009). This result corroborates the intrinsic fluorescence observations, thus showing that at these conditions, β-Lg is slightly unfolded, therefore either the tryptophan residues or the hydrophobic groups of β-Lg were less exposed, thus limiting the aggregation process.

Within heating treatments at pH 4, it was possible to obtain structures at macroscale (i.e., particles size ≥ 6 μm) for heating temperatures of 80 °C, independently of the β-Lg concentration used (Table 2). Under some combined conditions at 80 °C particles formed a sediment, which indicates that the protein at these conditions is completely unfolded, giving rise to the formation of aggregates. This can be also inferred by the high PDI value (i.e., PDI = 1), and the relatively high extrinsic fluorescence (i.e., ranging from 5.64 to 15.00) (Table 2) obtained, suggesting more hydrophobic sites available for ANS binding are exposed at these conditions (Schmitt et al., 2009). A similar behavior was also observed for intrinsic fluorescence with relatively higher intensity values recorded at this pH for 80 °C, in particular for 15 min holding time (Table 2); thus implying that tryptophan residues, originally buried in the interior of protein chain, are more exposed and so more likely to interact with bioactive molecules (He, Chen, & Moser, 2015).

At pH 4, which is relatively close to the pI of β-Lg, the net charge of protein is close to zero, and so the repulsive electrostatic forces weaken and the protein tends to aggregate, thus resulting in higher particle size values (Salgin, Salgin, & Bahadir, 2012). These observations agree with those reported by Leeb, Gotz, Letzel, Cheison, & Kulozik, 2015, which showed that β-Lg (5 mg mL^{-1}) prepared at pH 5.1 formed structures with particle sizes of 1332.1 ± 56.3 nm during thermal heating at 80 °C. In another study, Schmitt et al. (2009) obtained large aggregates with sizes above 1 μm for β-Lg at 1 mg mL^{-1} prepared at pH 4 and treated at 80 °C for 15 min.

At pH 6, when the temperature is taken to 80 °C, which is above the β-Lg denaturation temperature – i.e., 76 °C –, β-Lg is in a structural transition phase and so it is possible to obtain structures with particle size below and above 100 nm with relatively low PDI values – Table 2. In order to be able to draw accurate conclusions at this transition phase a full experiment was performed at pH 6 for these conditions for a heating temperature of 80 °C, and the combined effects of β-Lg concentration and holding time (Fig. 3) were evaluated to verify if these conditions were able to produce β-Lg structures with desired properties – i.e., particle sizes within micro- (between 200 and 300 nm) and nano- (≤ 100 nm) scales and with relatively low PDI values (i.e., ≤ 0.25).

In terms of particle size (Fig. 3A), β-Lg structures ranged from 65 nm to 267 nm with relatively constant surface charge (between −15.6 and −18.0 mV) ($p > 0.05$) (Fig. 3C), as β-Lg concentration or holding time increased. Results showed that β-Lg nanostructures (particles size ≤ 100 nm) can be obtained at 5 mg mL^{-1} for a heating time up to 25 min, at 10 mg mL^{-1} for a heating time up to 15 min and at 15 mg mL^{-1} for a holding time of 5 min, without statistically significant differences ($p \leq 0.05$) being found between particles size values. Results also show that large size particles (i.e., microstructures with sizes between 200 and 300 nm) can be obtained at 15 mg mL^{-1} for heating times ≥ 15 min. In fact, the effect of protein concentration and heating time on particles size has been already reported elsewhere (Bourbon et al., 2015; Hu, Yu, & Yao, 2007) for other proteins, which pointed to an increase in particles diameter with increased biopolymer concentration and heating time. Furthermore, it is possible to observe that β-Lg solutions present the best PDI values (≤ 0.25) when heated for time periods ≥ 15 min, independently of the β-Lg concentration used (Fig. 3B), thus suggesting that the aggregation process originated a relatively monodisperse particle size distribution (Schmitt et al., 2009).

According with previously published results, as pH moves away from the protein pI (i.e., between pH 5.2 and 7), β-Lg exhibits an increasing net charge on each molecule and it results in the presence of more dimers (with a molecular weight of approximately 36 700 Da, than monomers (with a molecular weight of 18 277 Da, and usually present at pH values below 3.0 or above 8.0), thus favoring the association and formation of structures with larger particle size (Png et al., 2009). This may be the reason for the higher particle size values observed for β-Lg at pH 6 than at pH 3 and 7, when heated at 80 °C – Table 2. This result agrees with a study conducted by Zúñiga, Tolkach, Kulozik, and Aguilera (2010), which showed the production of spherical aggregates with an average diameter of 96 nm at pH 6 and linear aggregates with an average diameter of 42 nm at pH 6.8.

The changes in the fluorescence intensity of the maximum intrinsic and extrinsic fluorescence spectra (λ_{max}) were used to follow structural changes of the protein induced by protein concentration and heating time at 80 °C. For intrinsic fluorescence an increase of fluorescence intensity at λ_{max} was observed as the heating time increased, particularly for periods ≥ 15 min (Fig. 3D). This difference in fluorescence intensity as a function of heating time may be related to changes in the compactness of the protein molecule due to local molecular unfolding, thus increasing the accessibility of buried tryptophan residues (Royer, 2006). This behavior has been also observed by Bourbon et al. (2015) for lactoferrin and lactoferrin-GMP nanohydrogels when heated at 80 °C up to 20 min and by Furtado et al. (2018) for lactoferrin solutions when heated at 90 °C up to 30 min. For extrinsic fluorencence (Fig. 3E) it is possible to see that an increase in heating time (from 5 to 25 min) was accompanied by a significant ($p \leq 0.05$) increase in the intensity of ANS fluorescence, independently of the β-Lg concentration used. This increase in extrinsic fluorescence intensity is in line with intrinsic fluorescence results.

Taking in consideration the best results obtained before, unheated β-Lg at 5, 10 and 15 mg mL^{-1} and heated β-Lg at 5, 10 and 15 mg mL^{-1} at 80 °C for heating times of 15 and 25 min were evaluated by circular dichroism in the far-UV region (from 190 to 260 nm) – Fig. 4. This technique was used to evaluate the influence of selected conditions of heating time in β-Lg secondary structure content in order to establish the best conditions to form structures at micro- (particle size between 200 and 300 nm) and nano- (particle size ≤ 100 nm) scales (Gorji et al., 2015).

The unheated β-Lg CD scans displayed a negative ellipticity minimum near 216 nm, suggesting that its structure is rich in β-sheet, which is consistent with previously reported results (Dave et al., 2013; Delahaije et al., 2016; Gomaa, Nsonzi, Sedman, & Ismail, 2016). Fig. 4 also shows an increase in the magnitude of ellipticity as β-Lg concentration increased. This technique is only sensitive to proteins that are fully-dissolved in the solution, so the increase in ellipticity intensity could be due to the fact that more protein is soluble with the increase in β-Lg concentration, consequently more amide chromophores of the peptide bonds can be measured by far–UV CD (Miles & Wallace, 2016). This result is in agreement with that reported by Ioannou, Donald, and Tromp (2015), which showed an increase in the magnitude of ellipticity as the concentration of β-Lg increased from 1 mg mL^{-1} to 40 mg mL^{-1}.

Regarding the thermal gelation process, a statistically significant difference ($p \leq 0.05$) is observed in the intensity of the negative peak of heated β-Lg in relation to the unheated β-Lg, independently of protein

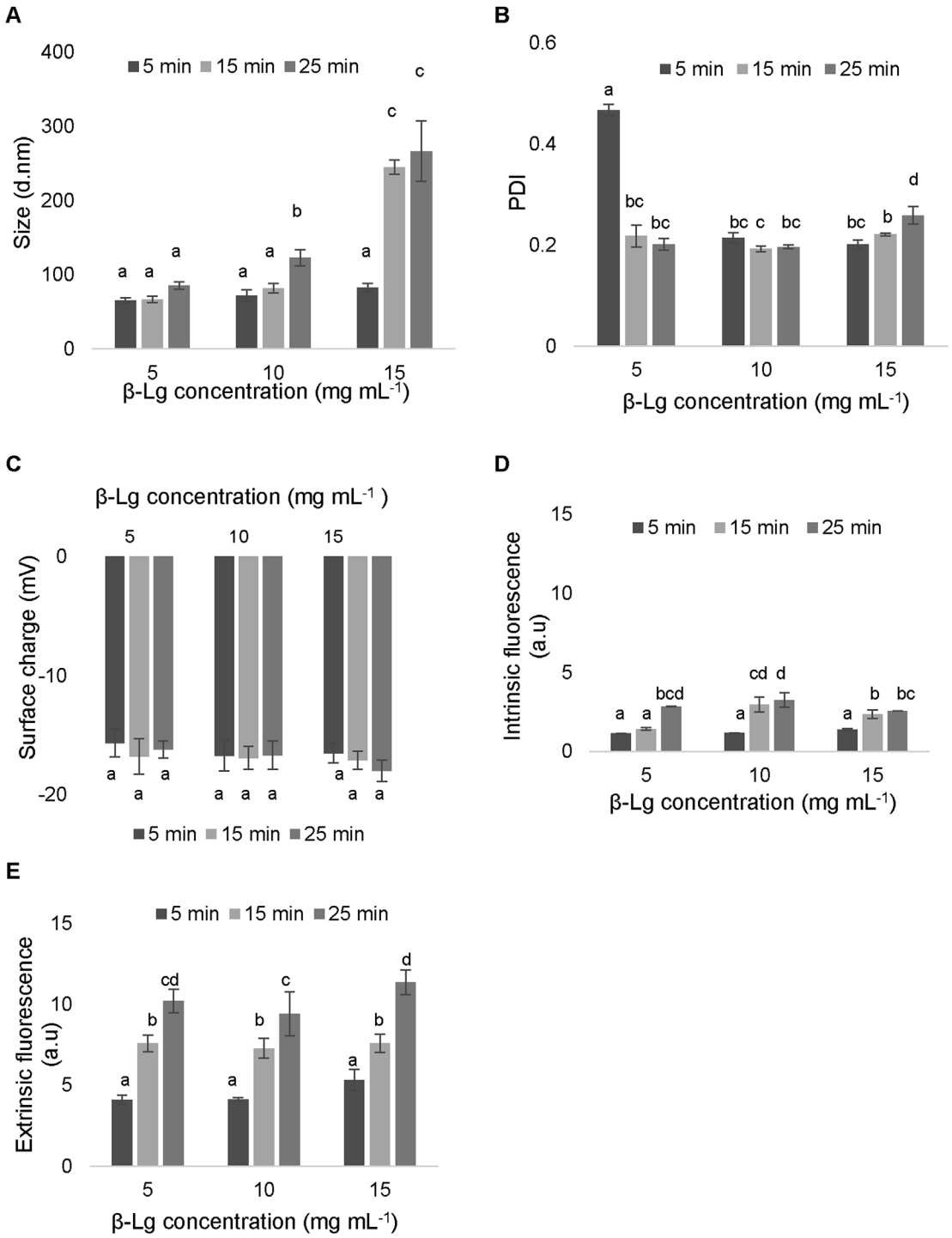

Fig. 3. Values of particle size (A), polydispersity (PDI) (B), surface charge (C), normalized maximum peak of intrinsic fluorescence at 295 nm (D) and normalized maximum peak of extrinsic fluorescence intensity at 370 nm (E) of β-Lg structures formed at pH 6 after heating at 80 °C for 5, 10 and 25 min at protein concentrations of 5, 10 and 15 mg mL^{-1}. Each data point is the average of nine successive measurements and the error bars show the standard deviation. Means labeled with the same letter do not statistically differ from each other ($p > 0.05$).

concentration. This can be related with structural changes due to aggregation phenomena (Jia, Gao, Hao, & Tang, 2017), which is consistent with intrinsic fluorescence data. Native β-Lg is characterized by having most of the hydrophobic amino acid residues buried inside the molecule (Wada, Fujita, & Kitabatake, 2006), so when the protein is subjected to thermal treatment, hydrophobic interactions responsible for maintaining the stability and conformational structure of β-Lg, may be disrupted, thus affecting β-Lg conformational state, resulting in loss of magnitude of the negative chirality of the CD signal (Ramos et al., 2015).

Simultaneously, β-Lg aggregation was accompanied by statistically significant differences ($p \leq 0.05$) in the red shift of zero-crossing, which suggests the formation of new regular secondary structures during thermal treatment. This result was in agreement with the data reported by Wada et al. (2006), which showed a CD spectra with a decrease of magnitude of the negative ellipticity for β-Lg heated at 80 °C when prepared at 0.5 mg mL^{-1} and at pH 7.5. These authors also observed a zero-crossing shift to shorter wavelengths, which have been

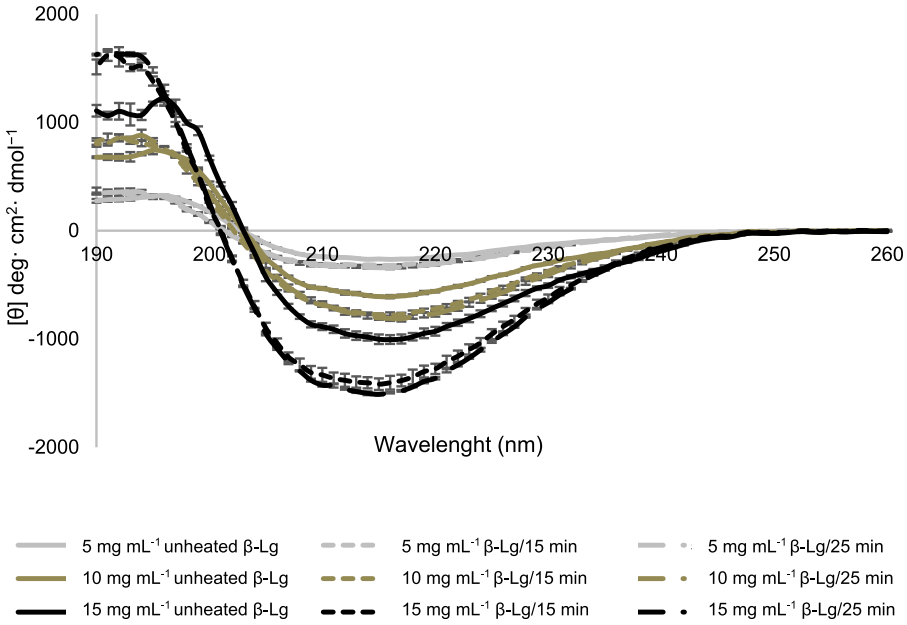

Fig. 4. Far-UV circular dichroism spectra of unheated β-Lg at 5, 10 and 15 mg mL^{-1} and heated β-Lg at 80 °C for 15 and 25 min for 5, 10 and 15 mg mL^{-1} at pH 6 (average ± standard deviation represented by error bars).

attributed to the increase α-helix structure content in the detriment of β-sheets content.

The results shown in Fig. 4 also indicate that heating time (15 and 25 min) did not significantly affect ($p > 0.05$) the negative signal intensity, independently of the β-Lg concentration used. These results are in accordance with DLS data, in which protein aggregation is shown to form structures without significance differences of particle size ($p > 0.05$), and are also in agreement with the data reported by Delahaije et al. (2016) when β-Lg at 20 mg mL^{-1} and at pH 7.0 was heated at 80 °C up 30 min, and by Dave et al. (2013) when β-Lg at 10 mg mL^{-1} and at pH 2 was heated at 80 °C up to 30 min. Both authors reported that the far-UV CD spectra of β-Lg heated at 80 °C remained approximately constant during heating time.

The morphology of β-Lg in its native state, and of micro- and nanostructures was observed by TEM and the respective microphotographs are provided as an insert in Fig. 5. Fig. 5A indicates that β-Lg in its native state is spherical and heterogeneous, with sizes ranging from 6.00 to 111.13 nm, which corroborate the high PDI value (> 0.36) obtained by DLS. This figure also shows aggregates form a black mass as a result of the negative staining procedure (Zúñiga et al., 2010). The particle size of β-Lg microstructures (Fig. 5B) as measured by TEM is around 140.8 nm, whereas DLS shown size values of 245.0 nm. It has been reported that differences between techniques for particle size measurement can be attributed to a sample drying effect for TEM analysis (Bourbon et al., 2016; Machado et al., 2012). However, β-Lg nanostructures (Fig. 5C) show a mean particle size of 61.6 nm, which corresponds well with DLS measurements. Micro- (Fig. 3B) and nanostructures (Fig. 3C) are uniform and homogenous, therefore the low PDI value (≤ 0.22) is well justified by the TEM images. Regarding micro- and nanostructures' shape, images do not reveal a visible and clear limit, but aggregates appear to be spherical and there seem to be clusters present. Clusters can be caused by the negative staining process, in which uranyl ions can be associated to β-Lg (Pinto et al., 2014). These features are consistent with TEM images obtained by Zúñiga et al. (2010) for β-Lg aggregates formed for protein concentration of 5 % w/v at pH 6, heated at 80 °C during 15 min.

4. Conclusions

β-Lg obtained from whey protein isolate was successfully purified and the method used is robust and reproducible. The purified β-Lg displayed identical physicochemical properties when compared with those exhibited by commercial β-Lg, which allows to use the purified β-Lg for the development of micro- and nanostructures. Experimental results at pH 3 and 7, independently of protein concentration, heating temperature and holding time, show that it is possible to produce structures with a particle size lower than 100 nm. Tryptophan fluorescence and surface hydrophobicity results suggest that the extent of unfolding and aggregation rate at those conditions are reduced due to the increase of electrostatic repulsion. Conversely, at pH 4 unstable structures were obtained, once this pH value is near the protein's pI.

Homogeneous and stable β-Lg micro- and nanostructures are formed at pH 6, after gelation process takes place at 80 °C (i.e., above β-Lg denaturation temperature) during 15 min: using β-Lg at 5 mg mL^{-1} and 15 mg mL^{-1} allows obtaining nano- and microscale structures with particles sizes of 70 nm and 250 nm, respectively. Furthermore, intrinsic and extrinsic fluorescence reveled structural changes and suitable environmental conditions to aggregation, while CD spectroscopy showed secondary structure changes with decrease of β-sheet and increase of α-helix contents.

The results obtained here represent a significant contribution to enrich the knowledge about the impact of several environmental conditions on β-Lg bio-based delivery systems' characteristics, and point at the possibility to tailor such characteristics as a function of the intended final application, e.g., in the food or pharmaceutical industries.

Acknowledgments

Lívia de Souza Simões gratefully acknowledges her grant to CNPq (Conselho Nacional de Desenvolvimento Científico e Tecnológico, Brasil) from Brazil. Oscar L. Ramos gratefully acknowledges the Fundação para a Ciência e Tecnologia (FCT, Portugal) for his fellowship (SFRH/BPD/80766/2011). The authors also would like to acknowledge Ana I. Bourbon, from the International Iberian Nanotechnology Laboratory, for assistance in native polyacrylamide gel electrophoresis. This study was supported by the FCT under the scope of the strategic

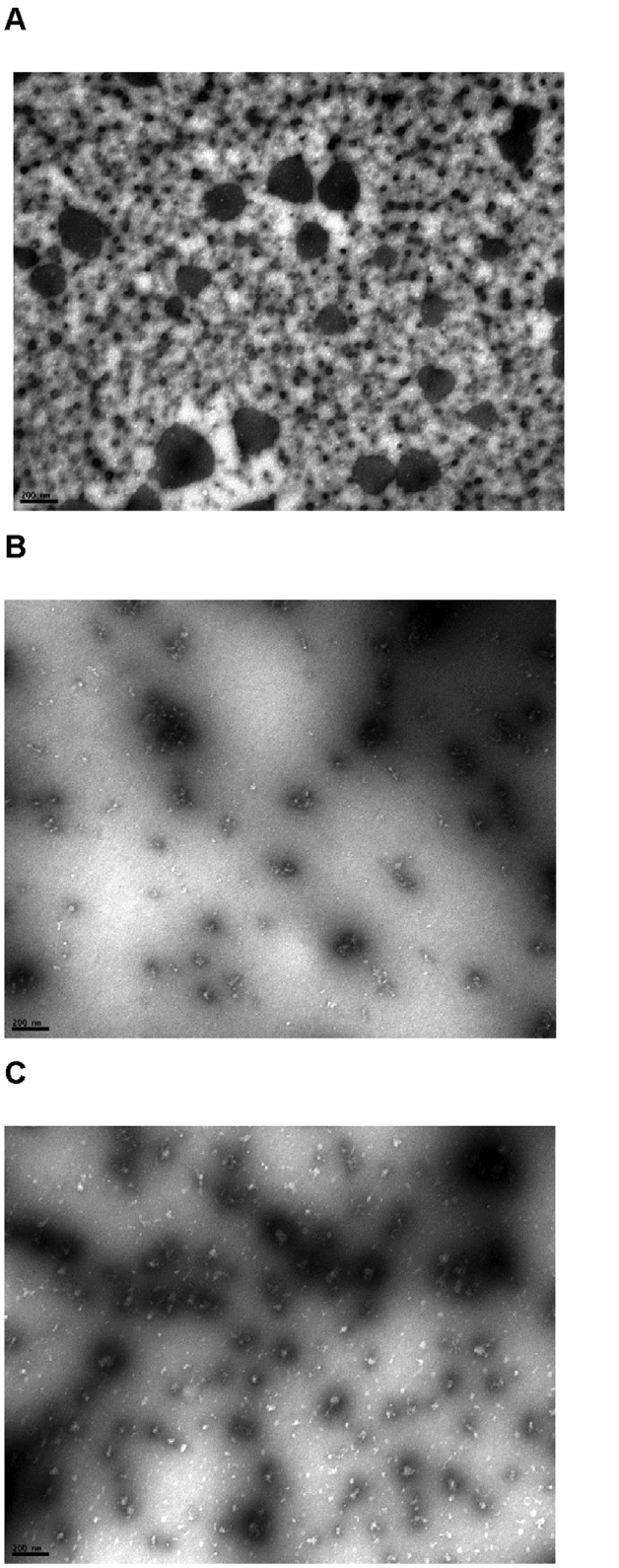

Fig. 5. TEM images of β-Lg native state A), β-Lg microstructures B), and β-Lg nanostructures C) (scale bar = 200 nm, magnification = 50.000×).

funding of UID/BIO/04469 unit and COMPETE 2020 (POCI-01-0145-FEDER-006684) and BioTecNorte operation (NORTE-01-0145-FEDER-000004) funded by the European Regional Development Fund under the scope of Norte2020 - Programa Operacional Regional do Norte, Portugal.

Appendix A. Supplementary data

Supplementary data to this article can be found online at https://doi.org/10.1016/j.foodhyd.2019.105357.

References

Aklakur, M., Rather, M. A., & Kumar, N. (2016). Nano delivery: An emerging avenue for nutraceuticals and drug delivery. *Critical Reviews in Food Science and Nutrition, 54*, 2317–2361. http://doi.org/10.1080/10408398.2013.839543.

Bourbon, A. I., Pinheiro, A. C., Carneiro-da-Cunha, M. G., Pereira, R. N., Cerqueira, M. A., & Vicente, A.a. (2015). Development and characterization of lactoferrin-GMP nanohydrogels: Evaluation of pH, ionic strength and temperature effect. *Food Hydrocolloids, 48*, 292–300. http://doi.org/10.1016/j.foodhyd.2015.02.026.

Bourbon, A. I., Pinheiro, A. C., Cerqueira, M. A., & Vicente, A. A. (2016). Influence of chitosan coating on protein-based nanohydrogels properties and *in vitro* gastric digestibility. *Food Hydrocolloids, 60*, 109–118. http://doi.org/10.1016/j.foodhyd.2016.03.002.

Dave, A. C., Loveday, S. M., Anema, S. G., Loo, T. S., Norris, G. E., Jameson, G. B., et al. (2013). β-lactoglobulin self-assembly: Structural changes in early stages and disulfide bonding in fibrils. *Journal of Agricultural and Food Chemistry, 61*(32), 7817–7828. http://doi.org/10.1021/jf401084f.

Delahaije, R. J. B. M., Gruppen, H., Van, E. L., Boxtel, E., Cornacchia, L., & Wierenga, P. A. (2016). Controlling the ratio between native-like, non-native-like, and aggregated β-lactoglobulin after heat treatment. *Journal of Agricultural and Food Chemistry, 64*, 4362–4370. http://doi.org/10.1021/acs.jafc.6b00816.

Delahaije, R. J. B. M., Wierenga, P. A., Giuseppin, M. L. F., & Gruppen, H. (2015). Comparison of heat-induced aggregation of globular proteins. *Journal of Agricultural and Food Chemistry, 63*(21), 5257–5265. http://doi.org/10.1021/acs.jafc.5b00927.

Diarrassouba, F., Liang, L., Remondetto, G., & Subirade, M. (2013). Nanocomplex formation between riboflavin and β-lactoglobulin: Spectroscopic investigation and biological characterization. *Food Research International, 52*(2), 557–567. http://doi.org/10.1016/j.foodres.2013.03.025.

Dombrowski, J., Gschwendtner, M., & Kulozik, U. (2017). Evaluation of structural characteristics determining surface and foaming properties of β-lactoglobulin aggregates. *Colloids and Surfaces A: Physicochemical and Engineering Aspects, 516*, 286–295. http://doi.org/10.1016/j.colsurfa.2016.12.045.

Dombrowski, J., Johler, F., Warncke, M., & Kulozik, U. (2016). Correlation between bulk characteristics of aggregated β-lactoglobulin and its surface and foaming properties. *Food Hydrocolloids, 61*, 318–328. http://doi.org/10.1016/j.foodhyd.2016.05.027.

Donato, L., Schmitt, C., Bovetto, L., & Rouvet, M. (2009). Mechanism of formation of stable heat-induced β-lactoglobulin microgels. *International Dairy Journal, 19*(5), 295–306. http://doi.org/10.1016/j.idairyj.2008.11.005.

Estévez, N., Fuciños, P., Bargiela, V., Picó, G., Valetti, N. W., Tovar, C. A., et al. (2017). Influence of pH on viscoelastic properties of heat-induced gels obtained with a β-Lactoglobulin fraction isolated from bovine milk whey hydrolysates. *Food Chemistry, 219*, 169–178. http://doi.org/10.1016/j.foodchem.2016.09.137.

Fan, L., Xie, P., Wang, Y., Liu, X., Li, Y., & Zhou, J. (2019). Influences of mannosylerythritol lipid-A on the self-assembling structure formation and functional properties of heat-induced β-lactoglobulin aggregates. *Food Hydrocolloids, 96*, 310–321. https://doi.org/10.1016/j.foodhyd.2019.05.033.

Fan, Y., Zhang, Y., Yokoyama, W., & Yi, J. (2017). β-Lactoglobulin-chlorogenic acid conjugate-based nanoparticles for delivery of (-)-epigallocatechin-3-gallate. *RSC Advances, 7*(35), 21366–21374. http://doi.org/10.1039/c6ra28462k.

Furtado, G. F., Pereira, R. N. C., Vicente, A. A., & Cunha, R. L. (2018). Cold gel-like emulsions of lactoferrin subjected to ohmic heating. *Food Research International, 103*, 371–379. 2017 http://doi.org/10.1016/j.foodres.2017.10.061.

Ghalandari, B., Divsalar, A., Saboury, A. A., & Parivar, K. (2015). β-Lactoglobulin nanoparticle as a chemotherapy agent carrier for oral drug delivery system. *Journal of the Iranian Chemical Society, 12*(4), 613–619. http://doi.org/10.1007/s13738-014-0519-2.

Gomaa, A. I., Nsonzi, F., Sedman, J., & Ismail, A. A. (2016). Enhanced unfolding of bovine β-lactoglobulin structure using microwave treatment: A multi-spectroscopic study. *Food Biophysics, 11*(4), 370–379. http://doi.org/10.1007/s11483-016-9451-6.

Gorji, E. G., Rocchi, E., Schleining, G., Bender-Bojalil, D., Furtmuller, P. G., Iturri, J. J., & Toca-Herrera, J. L. (2015). Characterization of resveratrol-milk protein interaction. *Journal of Food Engineering, 167*, 217–225. http://doi.org/10.1016/j.jfoodeng.2015.05.032.

Halder, U. C., Chakraborty, J., Das, N., & Bose, S. (2012). Tryptophan dynamics in the exploration of micro-conformational changes of refolded β-lactoglobulin after thermal exposure: A steady state and time-resolved fluorescence approach. *Journal of Photochemistry and Photobiology B: Biology, 109*, 50–57. http://doi.org/10.1016/j.jphotobiol.2012.01.005.

He, Z., Chen, J., & Moser, S. E. (2015). Interaction of β-lactoglobulin with (−)-epigallocatechin-3-gallate under different processing conditions of pH and temperature by the fluorescence quenching method. *European Food Research and Technology, 241*(3), 357–366. http://doi.org/10.1007/s00217-015-2466-2.

Hu, J., Yu, S., & Yao, P. (2007). Stable amphoteric nanogels made of ovalbumin and ovotransferrin via self-assembly. *Langmuir, 23*(11), 6358–6364. http://doi.org/10.1021/la063419x.

Ioannou, J. C., Donald, A. M., & Tromp, R. H. (2015). Characterising the secondary structure changes occurring in high density systems of BLG dissolved in aqueous pH 3 buffer. *Food Hydrocolloids, 46*, 216–225. http://doi.org/10.1016/j.foodhyd.2014.12.027.

Jia, J., Gao, X., Hao, M., & Tang, L. (2017). Comparison of binding interaction between β-lactoglobulin and three common polyphenols using multi-spectroscopy and modeling methods. *Food Chemistry, 228*, 143–151. http://doi.org/10.1016/j.foodchem.2017.01.131.

Konrad, G., Lieske, B., & Faber, W. (2000). A large-scale isolation of native β-lactoglobulin: Characterization of physicochemical properties and comparison with other methods. *International Dairy Journal, 10*(10), 713–721. http://doi.org/10.1016/S0958-6946(00)00099-6.

Kosters, H. A., Wierenga, P. A., De Vries, R., & Gruppen, H. (2011). Characteristics and effects of specific peptides on heat-induced aggregation of β-lactoglobulin. *Biomacromolecules, 12*(6), 2159–2170. http://doi.org/10.1021/bm2002285.

Leeb, E., Gotz, A., Letzel, T., Cheison, S. C., & Kulozik, U. (2015). Influence of denaturation and aggregation of β-lactoglobulin on its tryptic hydrolysis and the release of functional peptides. *Food Chemistry, 187*, 545–554. http://doi.org/10.1016/j.foodchem.2015.04.034.

Machado, A. H. E., Lundberg, D., Ribeiro, A. J., Veiga, F. J., Lindman, B., Miguel, M. G., et al. (2012). Preparation of calcium alginate nanoparticles using water-in-oil (W/O) nanoemulsions. *Langmuir, 28*(9), 4131–4141. http://doi.org/10.1021/la204944j.

Madadlou, A., Floury, J., Pezennec, S., & Dupont, D. (2018). Encapsulation of β-lactoglobulin within calcium carbonate microparticles and subsequent in situ fabrication of protein microparticles. *Food Hydrocolloids, 84*(March), 38–46. http://doi.org/10.1016/j.foodhyd.2018.05.054.

Madalena, D. A., Ramos, Ó., Pereira, R. N., Bourbon, A. I., Pinheiro, A. C., Malcata, F. X., et al. (2016). *In vitro* digestion and stability assessment of β-lactoglobulin/riboflavin nanostructures. *Food Hydrocolloids, 58*, 89–97. http://doi.org/10.1016/j.foodhyd.2016.02.015.

Maté, J. I., & Krochta, J. M. (1994). β-Lactoglobulin separation from whey protein isolate on a large scale. *Journal of Food Science, 59*(5), 111–114.

Miles, A. J., & Wallace, B. A. (2016). Circular dichroism spectroscopy of membrane proteins. *Chemical Society Reviews*. http://doi.org/10.1039/C5CS00084J.

Monteiro, A. A., Monteiro, M. R., Pereira, R. N., Diniz, R., Costa, A. R., Malcata, F. X., et al. (2016). Design of bio-based supramolecular structures through self-assembly of α-lactalbumin and lysozyme. *Food Hydrocolloids, 58*, 60–74. http://doi.org/10.1016/j.foodhyd.2016.02.009.

Pereira, R. N., Rodrigues, R. M., Ramos, Ó. L., Xavier Malcata, F., Teixeira, J. A., & Vicente, A. A. (2015). Production of whey protein-based aggregates under ohmic heating. *Food and Bioprocess Technology, 1–12*http://doi.org/10.1007/s11947-015-1651-4.

Perez, A. A., Andermatten, R. B., Rubiolo, A. C., & Santiago, L. G. (2014). β-Lactoglobulin heat-induced aggregates as carriers of polyunsaturated fatty acids. *Food Chemistry, 158*, 66–72. http://doi.org/10.1016/j.foodchem.2014.02.073.

Pinheiro, A. C., Bourbon, A. I., Cerqueira, M. A., Maricato, É., Nunes, C., Coimbra, M. A., & Vicente, A. A. (2015). Chitosan/fucoidan multilayer nanocapsules as a vehicle for controlled release of bioactive compounds. *Carbohydrate Polymers, 115*, 1–9. https://doi.org/10.1016/j.carbpol.2014.07.016.

Pinto, M. S., Léonil, J., Henry, G., Cauty, C., Carvalho, A. F., & Bouhallab, S. (2014). Heating and glycation of β-lactoglobulin and β-casein: Aggregation and *in vitro* digestion. *Food Research International, 55*, 70–76. http://doi.org/10.1016/j.foodres.2013.10.030.

Png, G. M., Falconer, R. J., Fischer, B. M., Zakaria, H. A., Mickan, S. P., Middelberg, A. P. J., & Abbott, D. (2009). Terahertz Spectroscopic Differentiation of Microstructures in Protein Gels. *Optical Society of America, 17*(15), https://doi.org/10.1364/OE.17.013102.

Ramos, O. L., Pereira, R. N., Martins, A., Rodrigues, R., Fuciños, C., Teixeira, J.a., et al. (2017). Design of whey protein nanostructures for incorporation and release of nutraceutical compounds in food. *Critical Reviews in Food Science and Nutrition, 57*(7), 1377–1393. http://doi.org/10.1080/10408398.2014.993749.

Ramos, O. L., Pereira, R. N., Rodrigues, R. M., Teixeira, J. A., Vicente, A. A., & Malcata, F. X. (2015). *Whey and whey powders: Production and uses. Encyclopedia of food and health* (1st ed.). Elsevier Ltdhttp://doi.org/10.1016/B978-0-12-384947-2.00747-9.

Ramos, O. L., Pereira, R. N., Rodrigues, R., Teixeira, J. A., Vicente, A. A., & Xavier Malcata, F. (2014). Physical effects upon whey protein aggregation for nano-coating production. *Food Research International, 66*, 344–355. http://doi.org/10.1016/j.foodres.2014.09.036.

Ramos, O. L., Pereira, J. O., Silva, S. I., Amorim, M. M., Fernandes, J. C., Lopes-da-Silva, J. A., et al. (2012). Effect of composition of commercial whey protein preparations upon gelation at various pH values. *Food Research International, 48*(2), 681–689. http://doi.org/10.1016/j.foodres.2012.06.004.

Rodrigues, R. M., Martins, A. J., Ramos, O. L., Malcata, F. X., Teixeira, J. A., Vicente, A. A., et al. (2015). Influence of moderate electric fields on gelation of whey protein isolate. *Food Hydrocolloids, 43*, 329–339. http://doi.org/10.1016/j.foodhyd.2014.06.002.

Royer, C. A. (2006). Probing protein folding and conformational transitions with fluorescence. *Chemistry Review, 106*, 1769–1784. http://doi.org/10.1108/SAMPJ-04-2014-0020.

Salgin, S., Salgin, U., & Bahadir, S. (2012). Zeta potentials and isoelectric points of biomolecules: The effects of ion types and ionic strengths. *International Journal of Electrochemical Science, 7*(12), 12404–12414.

Schmitt, C., Bovay, C., Vuilliomenet, A.-M., Rouvet, M., Bovetto, L., Barbar, R., et al. (2009). Multiscale characterization of individualized β-lactoglobulin microgels formed upon heat treatment under narrow pH range conditions. *Langmuir, 25*(14), 7899–7909. http://doi.org/10.1021/la900501n.

Simion, A.-M., Aprodu, I., Dumitraşcu, L., Bahrim, G. E., Alexe, P., & Stănciuc, N. (2015). Probing thermal stability of the β-lactoglobulin–oleic acid complex by fluorescence spectroscopy and molecular modeling. *Journal of Molecular Structure, 1095*, 26–33. http://doi.org/10.1016/j.molstruc.2015.04.019.

von Staszewski, M., Jara, F. L., Ruiz, A. L. T. G., Jagus, R. J., Carvalho, J. E., & Pilosof, A. M. R. (2012). Nanocomplex formation between β-lactoglobulin or caseinomacropeptide and green tea polyphenols: Impact on protein gelation and polyphenols antiproliferative activity. *Journal of Functional Foods, 4*(4), 800–809. http://doi.org/10.1016/j.jff.2012.05.008.

Stănciuc, N., Aprodu, I., Râpeanu, G., & Bahrim, G. (2012). Fluorescence spectroscopy and molecular modeling investigations on the thermally induced structural changes of bovine β-lactoglobulin. *Innovative Food Science & Emerging Technologies, 15*, 50–56. http://doi.org/10.1016/j.ifset.2012.03.001.

Teng, Z., Xu, R., & Wang, Q. (2015). Beta-lactoglobulin-based encapsulating systems as emerging bioavailability enhancers for nutraceuticals: A review. *RSC Advances, 5*(44), 35138–35154. http://doi.org/10.1039/C5RA01814E.

Vivian, J. T., & Callis, P. R. (2001). Mechanisms of tryptophan fluorescence shifts in proteins. *Biophysical Journal, 80*(5), 2093–2109. http://doi.org/10.1016/S0006-3495(01)76183-8.

Wada, R., Fujita, Y., & Kitabatake, N. (2006). Effects of heating at neutral and acid pH on the structure of β-lactoglobulin A revealed by differential scanning calorimetry and circular dichroism spectroscopy. *Biochimica et Biophysica Acta (BBA) - General Subjects, 1760*(6), 841–847. http://doi.org/10.1016/j.bbagen.2005.12.025.

Wang, W., Zhong, Q., & Hu, Z. (2013). Nanoscale understanding of thermal aggregation of whey protein pretreated by transglutaminase. *Journal of Agricultural and Food Chemistry, 61*(2), 435–446. http://doi.org/10.1021/jf304506n.

Yi, J., Lam, T. I., Yokoyama, W., Cheng, L. W., & Zhong, F. (2014). Controlled release of β-carotene in β-lactoglobulin – dextran-conjugated nanoparticles ' in vitro digestion and transport with caco - 2 monolayers. *Journal of Agricultural and Food Chemistry, 62*(35), 8900–8907.

Zúñiga, R. N., Tolkach, A., Kulozik, U., & Aguilera, J. M. (2010). Kinetics of formation and physicochemical characterization of thermally-induced β-Lactoglobulin aggregates. *Journal of Food Science, 75*(5)http://doi.org/10.1111/j.1750-3841.2010.01617.x.